Available online at www.sciencedirect.com
SCIENCE DIRECT®
Journal of Sound and Vibration 273 (2004) 713–740
JOURNAL OF SOUND AND VIBRATION
www.elsevier.com/locate/jsvi

Acoustic and seismic signals of heavy military vehicles for co-operative verification

J. Altmann[a,b,*]

[a] *Institut für Experimentalphysik III, Ruhr-Universität Bochum, D-44780 Bochum, Germany*
[b] *Experimentelle Physik III, Universität Dortmund, Dortmund, Germany*

Received 31 October 2002; accepted 7 May 2003

Abstract

To analyze the potential of ground sensors for co-operative verification, the Bochum Verification Project has measured sound and soil vibration produced by military vehicles. Both signals contain contributions from the engine which usually dominate in the acoustic channel. With tracked vehicles, the track produces additional components which dominate the seismic signal at close to medium range and render it more than ten-fold stronger than that of wheeled vehicles. The acoustic amplitude decreases roughly with the inverse distance, while keeping the signal shape. The seismic amplitude decreases faster, but shows local variations; the seismic signal shape varies strongly with position. Acoustic and seismic spectra consist mostly of harmonic line series, caused by the engine and, if present, the track. Acoustic and seismic sensors can detect heavy vehicles passively, independent of weather and daylight, at more than 100 m range. More complex tasks, such as vehicle-type recognition or trajectory determination, require further research.

1. Introduction

1.1. Verification by automatic sensor systems

Early arms control treaties concerned military systems which are large and/or fixed. Thus, verification of compliance could adequately be carried out by observation from outside. For disarmament treaties concerning small, mobile weapons, national technical means of verification—the most capable of which are only available for the U.S.A. and Russia anyway—have to be augmented by methods and technical means which work co-operatively, within national territory.

*Corresponding author.
E-mail address: altmann@ep3.ruhr-uni-bochum.de (J. Altmann).

0022-460X/$ - see front matter © 2003 Elsevier Ltd. All rights reserved.
doi:10.1016/j.jsv.2003.05.002

Co-operative verification, started in earnest in 1987, is done mainly by various types of on-site inspections [1], with the help of equipment which has grown in quality and quantity [2]. Most inspections are temporary spot-checks. Only in very few cases—for example the missile production facilities under the INF and START Treaties—has permanent presence of inspectors been agreed upon. Reluctance stems from the cost and intrusiveness connected with permanent human observation.

Automatic sensors deployed on site promise an alternative. The type and amount of information gained can be controlled in a transparent way. If effective, reliable and cost-efficient sensor-monitoring systems could be demonstrated, much more stringent limits on armed forces could be taken into consideration, including deeper cuts and/or changes to more defensive structures and postures. Concerning nuclear weapons, sensors could monitor transporter–erector–launcher vehicles of ballistic missiles, or sense missile launches in a co-operative early-warning system. A different area is peace-keeping. Here, agreed limits about cease-fire lines, weapons-free zones, etc. concern small and mobile systems as well as forces. At important roads crossing the designated lines, checkpoints can usually be staffed around the clock. The off-road portions of the lines, however, will at most be checked by occasional patrols, leaving many opportunities for unnoticed movement. Here, automatic ground-sensor systems deployed along the line would provide the first real possibility of continuous, gap-free monitoring. In a questionnaire survey, UN commanders and other peace-keeping officials responded positively to questions about the utility of ground sensors: more than 75% of the 114 respondents deemed ground sensors useful, and over 70% found them important [3]. An important precedent is provided by the monitoring of two mountain passes in the Sinai from 1976 to 1982 by the U.S.A. in the context of the armistice between Israel and Egypt [4,5].

Sensor monitoring relies on point and line controls [6–8]. The monitored area is defined by a boundary/perimeter line which may only be crossed by relevant vehicles at declared entry/exit points. At these, personnel and/or sophisticated short-range sensors will be used for detection, classification, and counting similar to the portal monitoring under the INF and START Treaties [2]. The rest of the designated line is declared off limits for treaty-limited equipment. Here, chains of medium-range ground sensors are deployed. On-site processors analyze the sensor data continuously; suspicious or unknown signals result in an alarm to a verification centre where human operators can send inspectors to the site to investigate the event, in case of a violation to try to prevent it or at least document it unambiguously, for example for later political decisions.

For the line sections between the checkpoints, cost and energy considerations lead to the requirements of passive detection without "illumination" of the target, working independent of daylight and in all weather conditions. For a low number of sensor sites, the detection range should be high. Cost and export-control reasons lead to the demand that the sensors should be cheap and commercially available. These criteria can be fulfilled by acoustic, seismic, and—in part—magnetic sensors. (Conventional highly sensitive magnetic sensors provide detection distances for heavy vehicles of several tens of metres; super-conducting sensors (SQUIDs) promise ranges well above 100 m [9].)

Since 1988, the Bochum Verification Project (BVP) at the Institut für Experimentalphysik III of the Ruhr-Universität Bochum, Bochum, Germany, has done research into the potential of acoustic, seismic, and magnetic automatic sensors for verifying limits on military land vehicles along control lines. This article reviews our results concerning acoustic and seismic signals.

1.2. Previous research

Land vehicles in operation are sources of sound and vibration, due to the running engine and to their own motion. Both the acoustic and the seismic excitations are produced by complex systems and interactions. The former is influenced, for example, by the engine inlet and exhaust geometries, the properties of tyre profile and the road surface, and by auxiliary systems such as compressors. The latter is influenced by the ground, the tyres or tracks, the suspension, and the vehicle body. In the course of efforts to understand and reduce driving noise, the *acoustic* emissions from several sources have been analyzed by measurements and modelling (e.g. Ref. [10,11]). Usually, this research has been directed towards noise reduction rather than detection of vehicles over a distance or classification of vehicle types.

With *seismic* excitation, the scientific literature contains even less information in these respects. One interest focuses on the prevention of road damage and thus concentrates on the dynamic forces below the tyres [12,13]. Propagation of vibration excitation to some distance has mainly been looked at in the context of preventing damage to buildings, which extends to several metres [10,14,15]. Vibration sensors, in particular geophones, can, however, detect levels smaller by several orders of magnitude and thus principally allow detection ranges much larger than those where building damage is expected.

Detection and classification of military vehicles is of course relevant in a military context, and in fact several highly industrialized countries have made studies using acoustic and seismic sensors; some even have fielded systems with their armies [16]. Since this research and the systems are directed to use in war (e.g., for monitoring the battlefield or the area behind the front, for triggering mines), the results and systems properties are generally kept secret. Where activities and systems are mentioned in publications at all, the information given is incomplete, vehicle types are not given, axes are not labelled, etc. (e.g. Refs. [17–19]).

It is for these reasons—different focus of the scientific literature, secrecy of similar work done in a military context—that the BVP had to carry out its own experiments with military land vehicles. Since the systems producing the excitation as well as the propagation processes are too complex to be easily modelled, an empirical approach was taken, first measuring signals under many different conditions.

The primary goals were to acquire acoustic, seismic and magnetic signals of moving military land vehicles at different distances. In order to contribute to confidence-building, the experiments were open. Scientists from several countries, including members of the former Warsaw Treaty Organization, took part from the beginning (see Table 1). To our knowledge, this is the first time that such measurements with military vehicles were allowed and carried out in an open, academic, international context. The BVP and the experiences gained from doing physics research for disarmament are described in Ref. [20].

For better understanding, some basic facts of vehicle signals and their propagation are to be mentioned: For heavy vehicles, the strongest source of acoustic excitation is the exhaust(s), followed by the intake(s). Noise from the engine, secondary systems, and power train is less important, the same holds for tyre and wind noise [10]. For tracked vehicles, the track mechanism provides additional acoustic sources, the strongest one is usually the drive sprocket wheel gripping into the gap between the track elements [21]. Acoustic excitation propagates as compressional wave with the speed of sound, with reflection and diffraction. Propagation above porous soil is

Table 1
Basic data of the land-vehicle experiments of the BVP

Time	Site Ref.	Road(s) Slope	Soil	Sensors, distance	Vehicles with number used	Approx. number passes	No. measurement sets; Recording	Scientists from
16–23 Aug. 1989	Doksy, Czech Republic [28]	Tarmac Level	Sand on sandstone	1 accelerometer (3D) 4.5 m 5–6 geophones 4.5–139 m 1–2 microphones 6–18 m	UAZ (small van, 1) Praga V3S (medium truck, 1) Tatra 815 (heavy truck with trailer for tank, 1) T 55 (main battle tank, 1)	110	1 analog tape	CZ, D
3–7 Dec. 1989	Baumholder, Germany [29]	Concrete (rough), terrain Sloped	Old lava with weathered layer	1 accelerometer (3D) 3.3 m 17 geophones 2.9–298 m (4 3D) 3 microphones 8.5–20 m 1 magneto-resistive sensor 6 m	Audi 200 (personal car, 1) VW 253 (van, 1) MB U 1300L (small truck, 1) MAN 630 (medium truck, 2) MD 220 (heavy truck with trailer for APC, 1) M 113 (armoured personnel carrier, 2) M 48 (main battle tank, 2)	150	3 ADC/computer/ hard disk; analog tape; analog tape	CZ, D, GB, F, NL, USA
10–14 Dec. 1990	Baumholder, Germany	Concrete (rough), terrain Sloped	Old lava with weathered layer	27 geophones 3.6–290 m (4 3D) 4 microphones 50 m 2 magneto-resistive sensors 6 m (1 3D)	MB 1017A (medium truck, 2) SLT 50-2 (heavy road tractor with trailer for tank, 2) M 113 (armoured personnel carrier, 2)	150	2 ADC/computer/ hard disk; analog tape	CZ, D, F, RUS, USA
12–17 Oct. 1992	Amersfoort, Netherlands [21]	Tarmac, terrain Level	Sand	30 geophones 3.1–200 m (1 3D) 12 microphones 3.1–200 m 4 magneto-resistive sensors 5–6 m (1 3D, 2 2D) 15 road-pressure sensors	DAF YA 4440 (medium truck, 2) DAF YTV 2300 (medium road tractor with trailer for APC, 1) MB 2648 (heavy road tractor with trailer for tank, 1) YPR 765 (armoured personnel carrier, 2) Leopard 1 (main battle tank, 2)	300	3 ADC/computer/ hard disk; ADC/computer/ hard disk; analog tape	CZ, D, GB, NL, RUS, USA

Sensor distances refer to the centre of the vehicle track on the hard road. For the complete information on local conditions, sensor types and layout, equipment and vehicles, see the references given. APC: armoured personnel carrier, ADC: analog-to-digital converter.

frequency and geometry dependent; it is described by the Weyl-van der Pol equation. In the atmosphere there are several additional effects, among them turbulence, refraction by temperature layering or wind shear [22,23].

Seismic signals are much more complicated. Direct seismic excitation is produced by time-varying forces exerted by the vehicle on the ground. Such forces can be a consequence of the road roughness or the tyre profile; particularly strong ground vibration is produced by tracked vehicles the tracks of which can be seen as an unusually rough road with periodic bumps. In case of a more or less constant spatial period L, the vertical wheel motion is similar to a forced vibration at the frequency $\nu = v/L$, where v is the vehicle speed. In case of aperiodic excitation, for example by a single bump, the vehicle reacts by elastic, damped vibration at characteristic frequencies or frequency bands given by the properties of the tyres, the suspension, and the vehicle body. Typical eigenfrequencies for trucks are: the basic tyre mode (tyre against rim): 30–60 Hz; motion of the wheel suspension between ground and vehicle body: 10–20 Hz; vibration of the body: 1–3 Hz [24].

Seismic excitation produces different wave types (in the volume, compressive (p) and shear (S) waves; near the surface, two shear waves of the Rayleigh and Love type, respectively) which all propagate with different velocities [25]. Due to spherical or circular propagation, the amplitude decrease with distance is proportional to r^{-1} for volume, and $r^{-1/2}$ for surface waves. In case of layered soil, surface waves exhibit dispersion, i.e., components of different frequencies travel with different speeds, thus their superposition and the resulting wave form and amplitude vary with distance. Vertical vibration at the surface should consist mainly of Rayleigh waves. Finally, the absorption of seismic waves increases strongly with frequency; in sediment which is of main interest here, typical ranges of the absorption coefficient are 10^{-4}–10^{-2}/m at tens of Hz and 10^{-2}–1/m at few hundred Hz [26]. Thus, seismically propagating frequencies above 100 Hz can decrease by orders of magnitude over tens of metres.

Seismic excitation is also produced indirectly when sound waves travel along the ground. This effect is stronger with soft, porous soil than with a single hard surface (rock, ice). In the former case, the varying air pressure produces a slow acoustic wave travelling nearly vertically into the soil pores. Friction then sets the soil matrix into motion; this is usually treated as a local effect [27]. Acoustic-seismic transfer leads to soil vibration at acoustic-noise frequencies, with ensuing seismic propagation. The total seismic signal is a superposition of the various direct and indirect contributions.

1.3. Goals of this article

This paper is intended to inform about the experiences and elementary evaluations made with acoustic and seismic signals of heavy military land vehicles. Basic information and numbers are to be provided which have up to now not been easily accessible or even not published at all. Details of the author's experiments are described in the Verification—Research Reports [21,28,29].

The remaining sections are as follows: After a short outline of the land-vehicle experiments of the BVP in Section 2, a few example sensor signals are presented in Section 3. Acoustic and seismic amplitudes of different vehicles are discussed as they depend on distance and speed, and rough estimates on detection distances are given (Section 4). Typical acoustic and seismic spectra are shown and explained in Section 5, in particular the main harmonic series and its strongest member. Two special aspects are treated in Section 6: sensor-array processing and seismic signals

from a bump in the road. Finally Section 7 presents conclusions and recommendations for further progress.

2. Land-vehicle experiments of the BVP

Between 1989 and 2000, the BVP carried out six open experiments (four of them international) measuring military land vehicles. Only the four land-vehicle experiments where sensors were deployed at many distances will be discussed here (Table 1). (The other measurements dealt with a standing tank and with vehicles passing between two sensor stations [30].)

The measurements focused on heavy military vehicles, which are predominantly main battle tanks (MBT) and armoured personnel carriers (APC). Since both can be transported by road tractors (this is the normal way of moving them over larger distances, but could also be used to fool a sensor system), such vehicles were included, too. For comparison and because they have an important military role as well, trucks of different size were also measured.

Two of the three measurement sites were military training grounds with some background activity at times. The first experiment at Doksy with 11 channels served mainly to gain basic information on signal strengths, decrease with distance, and spectral content. The later measurements used light-beam interruption devices to measure the vehicle movement and employed more sensors. Most of them were placed in a line perpendicular to the road in order to measure the acoustic- and seismic-wave propagation with distance. Others were placed in an array for evaluations regarding finding the direction of a vehicle. At important locations microphones and geophones were placed together to measure the acoustic-to-seismic coupling. Some geophones were buried to assess the influence of depth. Most of the geophones sensed vertical soil velocity; at a few locations, three-dimensionally sensitive combinations were used. Only vertical vibration will be considered here, for three-dimensional motion see Ref. [29]. Fig. 1 shows the sensor layout of the most comprehensive experiment at Amersfoort, Netherlands, 1992. It is the source for all figures shown below (except Fig. 7a).

Power was provided by truck batteries and AC converters, in some cases by a combustion-engine-powered generator. Whereas in the first experiment in 1989 at Doksy only one recording system was used and all signals were recorded on multi-channel analogue tape, from the second one, two or three separate sensing and recording systems were operating, and at least one system of the BVP used direct analog-to-digital conversion (12 bits resolution) under control of a personal computer with immediate data storage to hard disk. Analog-tape data were digitized off line, and all digital measurement files were archived on write-once, read-multiply (WORM) optical disks. Most evaluations were done with the data from the main digital BVP measurement set.

Table 2 gives a few specifications of typical sensors used. Sensor signals were low-pass filtered and amplified, with gains set by hand switches. Amplifiers, filters, etc. were either commercial or built in the respective institutes. The recording bands were usually limited at the low end by the sensors: microphones about 3 or 20 Hz, geophones mostly about 3 Hz. At the high end, electronic filters were used. For microphones, the 3-dB frequencies were often 1 kHz, sometimes 300 Hz or up to 10 kHz. Geophone signals were filtered at 300 Hz usually; very few sensors were limited below, e.g., at 80 Hz. Digital sampling rates were at least 2.5–3 times the filter frequencies.

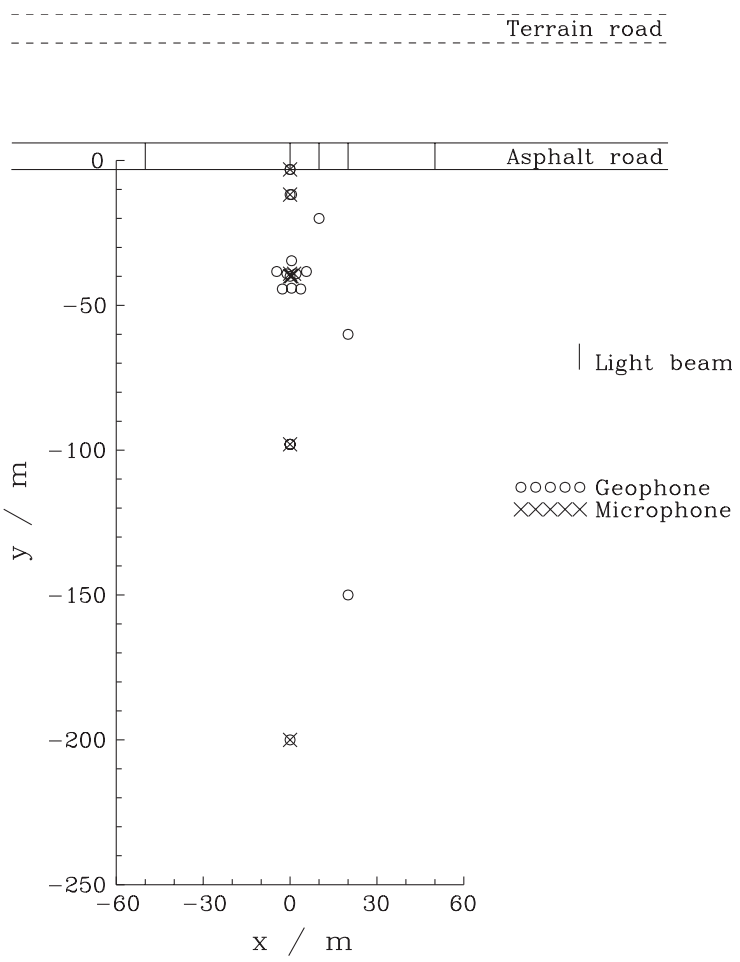

Fig. 1. Layout of the sensor positions during most of the Amersfoort 1992 measurements. Along the asphalt road, five light-beam interruption devices serve to determine the trajectory of the vehicle in the x direction. For convenience, the positive x direction (60° from geographic North) is denoted "east", the opposite "west".

Table 2
Specifications of a few sensor types used in the experiments

Microphone	Brüel & Kjaer 4165 with 2639 preamplifier, frequency range 2.6 Hz–20 kHz, sensitivity 50 mV/Pa
Microphone	Sennheiser KE-4-211-2, frequency range 20 Hz–20 kHz, sensitivity 10 mV/Pa
Geophone	Sensor Nederland SM-6, eigenfrequency 4.5 Hz, sensitivity 26 V/(m/s), vertical and horizontal

For space reasons, only the most important data are shown. Typical cut-off frequencies of the low-pass filters in the amplifiers were 0.3 kHz for geophones and 1 kHz for microphones.

Evaluations have shown that for heavy vehicles, a recording band between a few Hz and few hundred Hz contains the overwhelming part of the seismic-signal energy. The acoustic energy is mostly between 20 Hz and 1 kHz, with the major portion below a few hundred Hz (see also Fig. 8).

Table 3
Basic specifications of the vehicle types used in the Amersfoort 1992 experiment

Type	Class	Total mass empty (Mg)	Length (m)	No. axles/ roller wheels per side	Engine class, exhausts	Power (kW)
DAF YA 4440	Medium truck	7.0	7.2	2	L 6 D 4, 1	109
DAF YTV 2300	Medium road tractor (for APC)	7.9 + ~10	16.5	2+2	L 6 D 4, 1	180
MB 2648	Heavy road tractor (for MBT)	~15 + 23.0	20.0	3+6[a]	V 8 D 4, 2	362
YPR 765	APC	11.4	5.3	5	V 6 D 2, 1	196
Leopard 1	MBT	40.5	7.1[b]	7	V 10 D 4, 2	610

Class: APC: armoured personnel carrier, MBT: main battle tank. Engine: L/V: in-line/V-type cylinder arrangement, number of cylinders, P/D: petrol/Diesel, number of strokes, number of exhausts.
[a] The foremost two axles of the trailer can be raised without load.
[b] Excluding gun.

Table 3 shows specifications of the vehicles used at Amersfoort. Usually, measurement runs were done over about 400 m, 200 m on each side of the main sensor line. Drivers were instructed to keep a certain speed, with nominal values of 5, 20, and 40 km/h in all experiments, and intermediate values at 5-km/h steps in the Amersfoort experiment. They did not drive exactly with the nominal speed, but usually kept the speed constant during each run. Various types of special measurements were done in addition, among them passes with bumps on the road, passes using non-linear paths, and standing-vehicle running-engine measurements.

3. Example sensor signals

General properties of amplitude time courses are demonstrated in Fig. 2 which shows signals from microphones and geophones at various distances (3.1–98 m from the lane centre) while a main battle tank Leopard 1 passed between $x = -100$ and $x = 100$ m. A tank produces very strong signals. At the farthest sensor and the beginning of the interval, the acoustic amplitude is more than one order of magnitude above the background, the seismic one nearly three (see Section 4.2). The maximum amplitudes are higher at the closer sensors, and there is a general amplitude increase as the vehicle approaches the sensor line ($x = 0$ m), and a decrease as it moves away again. The relative amplitude variation during a pass is highest at the closest sensors which reflects the highest relative variation of vehicle-sensor distance there. That the amplitudes are often higher after passing is probably due to some directivity of the acoustic emission, since the major sources (exhausts) are at the rear.

Fig. 3 shows sections of the acoustic and seismic signals at 11.8 m from the lane centre when the tank just passed the $x = 0$ m position. These signals have not much in common. Clearly the acoustic one (a) is dominated by the engine, as a result of sound emitted from the exhausts. The signal is more or less periodic with a period of about 51 ms. The seismic signal (b) is markedly different. There is no clear periodicity. Counting the major peaks or troughs leads to a dominant contribution of about 21 ms period.

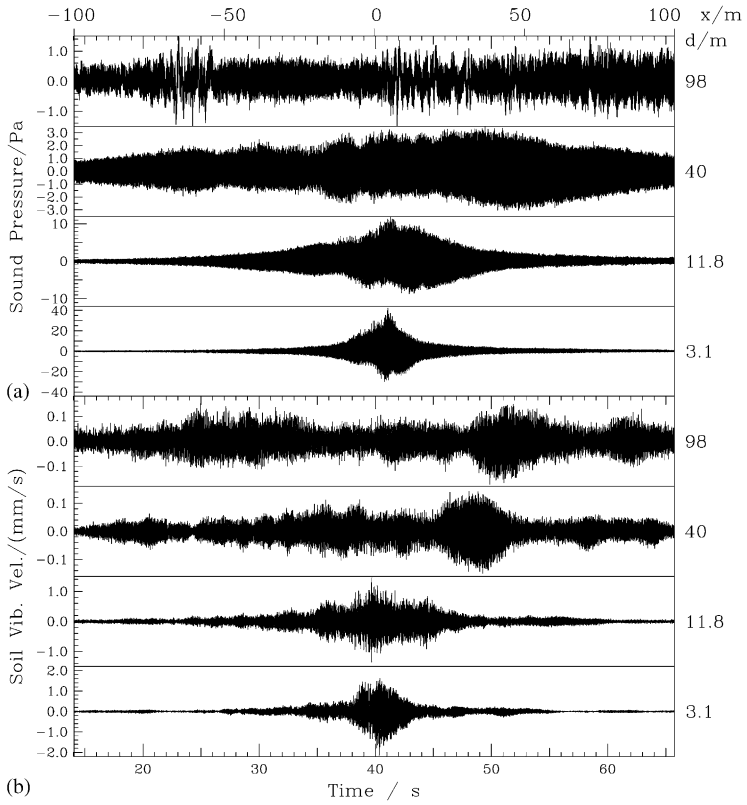

Fig. 2. Acoustic (a) and vertical seismic (b) signals during a pass of a Leopard-1 main battle tank with 3.9 m/s (direction east). The sensor distance from the zero point is indicated on the right. The position along the road (x) is shown at the top; the vehicle centre passed the zero point at $t_0 = 40.2$ s. Filter frequencies acoustic 300 Hz, at 3.1 m 1 kHz; seismic 300 Hz, at 98 m 80 Hz.

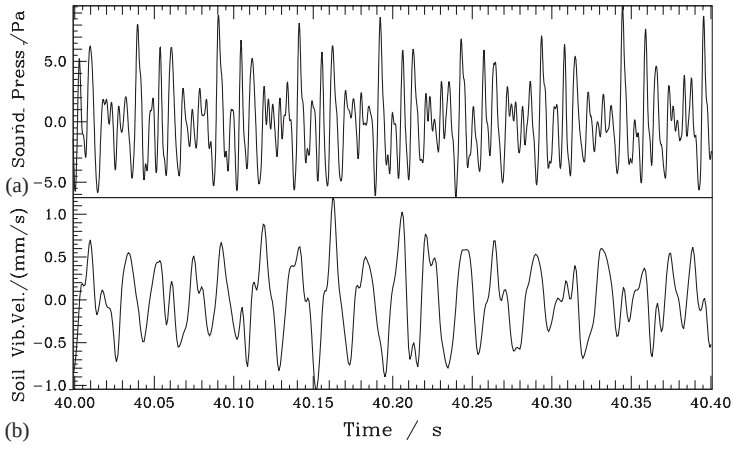

Fig. 3. Sections from acoustic (a) and vertical seismic (b) signals at 11.8 m distance when a Leopard-1 main battle tank just passed the sensor line ($x = 0$ m, at 40.2 s). The pass is the one of Fig. 2. Filter frequencies: 300 Hz both channels.

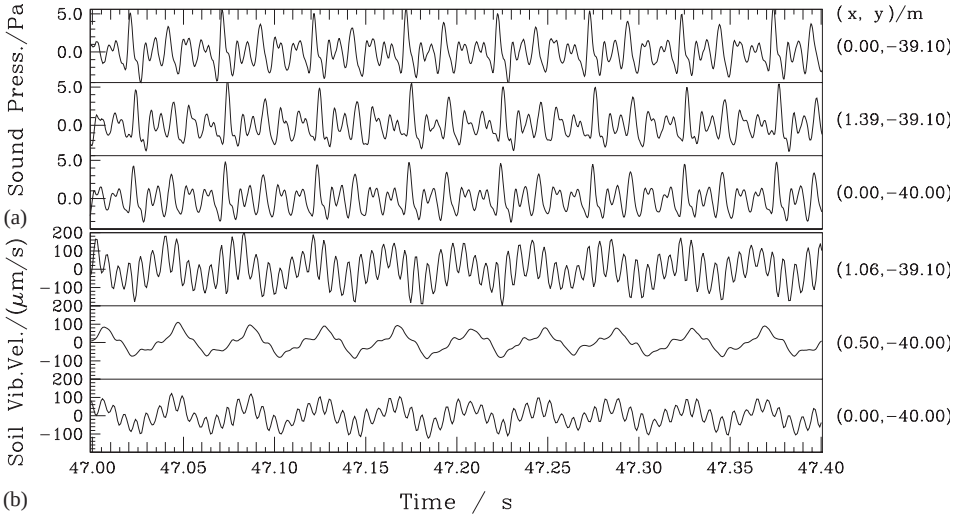

Fig. 4. Similarity and dissimilarity of signals at adjacent sensors, about 40 m from the lane. Shown are three acoustic (a) and three vertical seismic (b) signals measured during a pass of a Leopard-1 main battle tank with −4.1 m/s (direction west), when the vehicle passed at $x = -45$ m (sensors in the left rear, the zero point had been passed at $t_0 = 36.1$ s). The sensor co-ordinates are given on the right. Filter frequencies acoustic 1 kHz, seismic 300 Hz.

Seismic signals are more variable than acoustic ones not only temporally, but also spatially. Fig. 4 shows simultaneous signals at neighbouring microphones and geophones about 40 m from the road; all were within 2 m distance. The acoustic signals (a) are very similar—they are practically time-shifted versions of each other, with cross-correlation coefficients of 0.95 and above; the time shifts of the correlation maxima fit to the propagation-path differences, as expected for a single wave type with a frequency-independent velocity, namely the sound velocity. (Note that with multiple sources, sometimes neighbouring-sensor signals did differ.)

On the other hand, the seismic signals (b) show impressive variations of shape. All signals contain a low-frequency contribution of about 25 Hz of about similar strength which is the track frequency. Striking is the varying content at the high frequency, 158 Hz: it cannot be seen in the centre signal, whereas in the upper one it is more than double the lower. This is the eighth multiple of the engine frequency which stems from acoustic-seismic transfer. Obviously this transfer varies strongly between positions less than 1 m apart. Other reasons for spatial variations can be dispersion of Rayleigh surface waves, soil inhomogeneity, and multiple sources. The cross-correlation coefficients are often 0.5 and lower, and the time shifts of relative best fits are generally not consistent with propagation at one wave velocity. This effect is generally observed; it makes beam-forming and other sensor-array computations difficult for seismic signals (see Section 6.1).

4. Amplitudes

4.1. Peak amplitudes

In order to give an idea of the amplitudes near the source, Table 4 lists approximate maximum values of the sound pressure and the soil vibration velocity as measured at the sensors directly at

Table 4
Rough maximum values of sound pressure and vertical soil vibration amplitudes at 3–5 m distance from the vehicle centre at speeds between 20 and 40 km/h (time domain, linear, few Hz to 0.3 or 1 kHz)

Source	Peak sound pressure (Pa)	Peak sound pressure level (dB re. 20 μPa)	Peak seismic velocity (m/s)	Peak seismic velocity level (dB re. 1 m/s)
Personal car	—	—	1×10^{-4}	−80
Small truck	6×10^{0}	110	2×10^{-4}	−74
Medium truck	1×10^{1}	114	1×10^{-3}	−60
Heavy truck	1×10^{1}	114	1×10^{-3}	−60
Armoured personnel carrier	3×10^{1}	124	1×10^{-2}	−40
Main battle tank	8×10^{1}	132	2×10^{-2}	−34

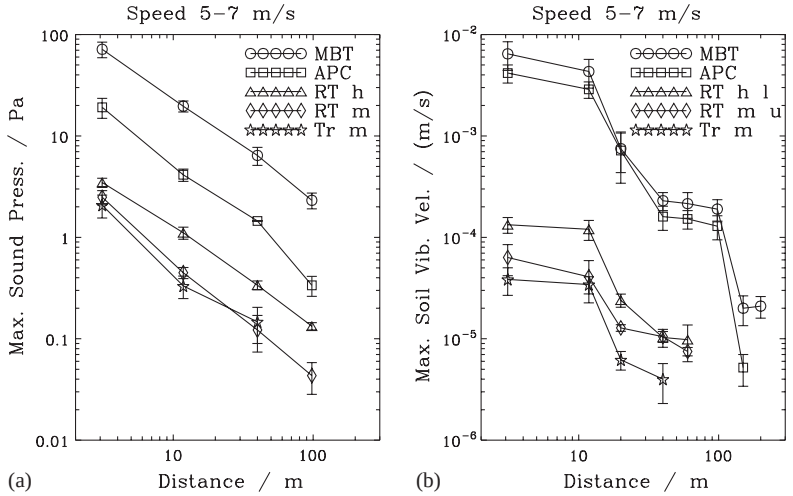

Fig. 5. Maximum values of sound pressure (a) and vertical soil vibration velocity (b) during passing versus distance from the lane centre, for heavy military vehicles driving with 5–7 m/s speed, occurring within ±5 s around passing of the sensor line, average and standard deviation of 2–13 values each. Filter frequencies acoustic 300 Hz and 1 kHz, seismic 300 Hz (98 m: 80 Hz). MBT: main battle tank Leopard 1 (2 vehicles); APC: armoured personnel carrier YPR 765 (2 vehicles); RT h (l): heavy road tractor Mercedes-Benz 2648, (1 vehicle); (a): loaded and unloaded; (b): loaded only; RT m (u): medium road tractor DAF YTV 2300 (1 vehicle); (a): loaded and unloaded; (b): unloaded only; Tr m: medium truck DAF YA 4440 (2 vehicles).

the road margin, i.e., at 3–5 m from the vehicle centre when it passed the sensor line. For comparison: With no unusual activity in the vicinity and moderate wind speeds, the acoustic background is below 10^{-2} Pa, the seismic one is a few times 10^{-7} m/s. The human sensitivity threshold for sound is 2×10^{-5} Pa at 1 kHz, for vibration (vertical, whole-body) it is about 3×10^{-4} m/s at tens of Hertz [31,32]. For the non-sinusoidal vehicle signals, r.m.s. values were generally about one-third of the absolute maximum values.

For the amplitude dependence on distance and speed, the absolute maximum values occurring in a 10-s interval around the time when the vehicle passed the sensor line were determined for the

Amersfoort passes at all distances (excluding signals masked by background noise, etc.). Fig. 5a shows the distance dependence of the peak sound pressure for all vehicles, when driving with speeds between 5 and 7 m/s, on a double-logarithmic scale. The amplitude at fixed distance is mainly a function of engine size (and rotation rate, not visible here). For tracked vehicles, track-related noise contributes significantly. For the armoured personnel carrier with its smaller engine, the track noise is stronger than the engine one, whereas for the tank the engine sound dominates by far [21]. The overall noise amplitude increases from the medium truck via the heavy road tractor and the armoured personnel carrier to the main battle tank by factors of 2–3, 3–4, and 4–5, respectively. Because there was no discernible difference in sound amplitudes when the road tractors drove with or without load, both kinds of passes are included in Fig. 5a.

Optimal power-law fits have exponents between -1.16 and -0.94, similar to the $1/r$ amplitude decrease with distance expected for unattenuated propagation from a point source into free (half) space with still air. Note, however, that the maximum sound pressure occurred at some time within the 10-s interval, mostly not at the time of closest approach, and the $1/r$ decrease does not hold for momentary (retarded) propagation, see also the variations with time in Fig. 2. One of the reasons for deviations from point-source propagation is probably that there are several acoustic sources, together with diffraction around the vehicle body. Wind-induced variations should be less important under the Amersfoort conditions; frequency-dependent attenuation due to the porous ground is not visible in this summary presentation.

Fig. 5b shows the dependence of the maximum soil vibration velocity on distance for the same vehicle types, again at speeds of 5–7 m/s. For clarity of presentation, only heavy-road-tractor passes with, and medium-road-tractor passes without load are shown (see Fig. 7b). The general shape of the curves is similar for all vehicle types. Evidently the vehicles form two main groups, namely tracked and wheeled ones, with the former 1.5 orders of magnitude stronger than the latter. (Mainly due to noise from background vehicles, reliable amplitude values of the wheeled vehicles are unfortunately not available for large distances.) While there is a general decrease with distance, it is not at all similar to a simple power law as might be expected, as for example with a monochromatic seismic surface or volume wave from a point source where exponents of -0.5 resp. -1 would hold in the far field.

For determining an optimally fitting exponent, one should remove the close geophone at 3.1 m distance from the lane centre which was still on asphalt. The road is stiffer than the surrounding soil, thus its deflection will comprise a larger area with less amplitude. With the remaining points, power-law fits resulted in distance exponents of -2.0 to -0.9, average -1.6.

For possible explanations of the irregularities, one can point to local variations. At the 98-m position for example, there were indications for unusually high acoustic-seismic transfer. Another plausible explanation is seismic attenuation which affects the higher frequencies most strongly. One can also speculate as to whether the multiple sources (here, 14 road wheels) lead to partial cancellation of signals. Detailed understanding would require relatively complex measurements using single, fixed, acoustic as well as seismic sources. Mainly due to time constraints, such investigations could not be performed during the vehicle experiments. Lacking full understanding, a useful heuristic description may be that the maximum seismic amplitude—on the soil, excluding the road part—shows a general decrease between $r^{-1.5}$ and r^{-2} to about 200 m, but may be modified by as much as an order of magnitude or more depending on local factors.

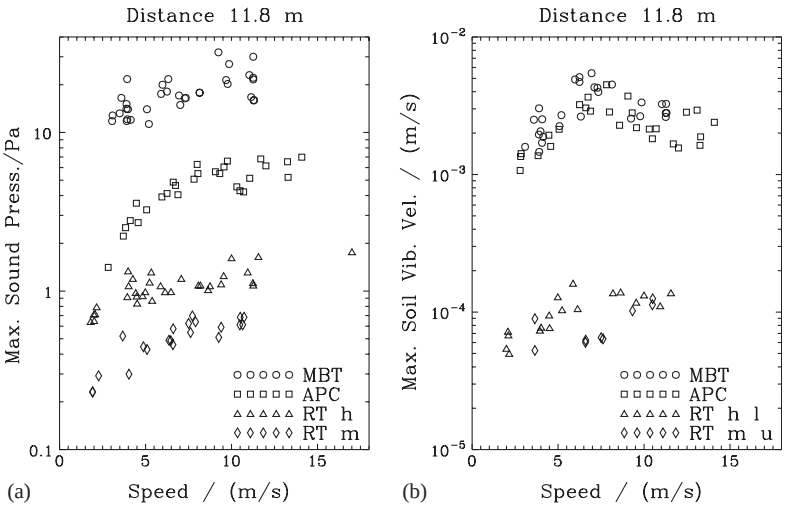

Fig. 6. Maximum values of sound pressure (a) and vertical soil vibration velocity (b) during passing versus vehicle speed, at 11.8 m distance from the lane centre, occurring within ± 5 s around passing of the sensor line, individual passes. Filter frequencies acoustic 300 Hz and 1 kHz, seismic 300 Hz. MBT: main battle tank Leopard 1 (2 vehicles); APC: armoured personnel carrier YPR 765 (2 vehicles); RT h (l): heavy road tractor Mercedes-Benz 2648, (1 vehicle); (a): loaded and unloaded; (b): loaded only; RT m (u): medium road tractor DAF YTV 2300 (1 vehicle); (a): loaded and unloaded; (b): unloaded only. Data of the medium truck (DAF YA 4440) are in the same range (not shown).

Fig. 6a shows the dependence of the maximum acoustic amplitude on vehicle speed at a fixed distance of 11.8 m. Road-tractor passes with and without load are included. For clarity of presentation, medium-truck data are not shown—they are in the same range as those of the medium road tractor. Except for the armoured personnel carrier, there is considerable scatter. The acoustic amplitude generally increases with speed, reaching a plateau at about 10 m/s. Not surprisingly, the general amplitude level increases with engine size. Because of the large scatter, amplitude dips, expected at speeds where the drivers would switch to a higher gear with a lower rotation rate, are not seen clearly.

The dependence of maximum seismic amplitude on vehicle speed at 11.8 m distance is shown in Fig. 6b. For clarity of presentation, only heavy-road-tractor passes with, and medium-road-tractor passes without load are shown (see Fig. 7b for the differences between unloaded and loaded vehicles). Also here, data vary considerably between passes of the same vehicle type. As in Fig. 5b, tracked vehicles are about 1.5 orders of magnitude stronger than heavy wheeled ones. Whereas the soil vibration from the armoured personnel carrier is slightly less than that of the main battle tank on average, both distributions overlap significantly. The data of the wheeled vehicles are consistent with a linear dependence on speed, as in an empirical formula for a single bump and measurements at a rough stone-paved road [14,15]. For the tracked vehicles, on the other hand, there seems to be a maximum of seismic amplitude around 6–8 m/s.

A few additional results with seismic amplitudes shall be mentioned in brief. Fig. 7a compares peak seismic amplitudes of three types of main battle tanks observed during passes with about 20 km/h speed at three different sites, on hard as well as terrain roads, with or without rubber pads on the track. It is interesting that at close and medium distances, all amplitudes agree within

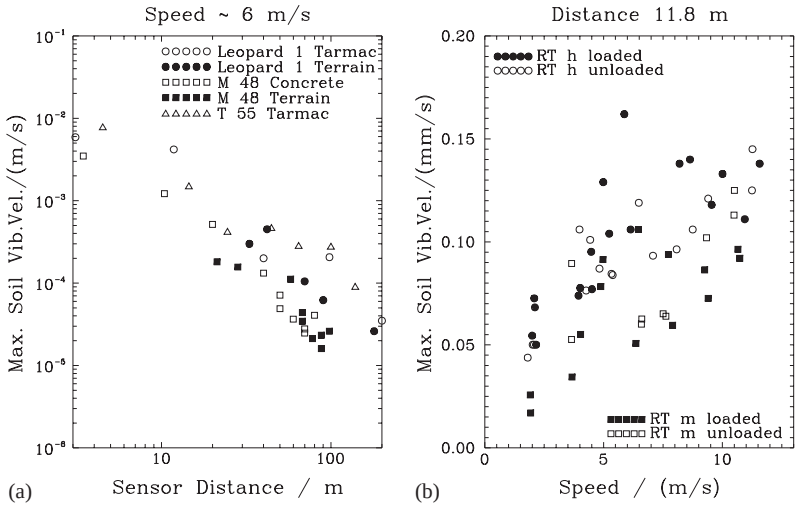

Fig. 7. Similarity and variability of seismic amplitude under different conditions. Filter frequencies mostly 300 Hz, few points 80 Hz. (a) Peak values of vertical soil vibration velocity versus distance for main battle tanks of different types, driving on different soils and road types, with (M48, Leopard 1) or without (T 55) rubber pads on track, observed during passes with about 20 km/h (5.6 m/s). Experiments: Doksy (T 55), Baumholder 1989 (M48), Amersfoort (Leopard 1). (b) Peak values of vertical soil vibration velocity versus speed at 11.8 m distance from the lane centre, occurring within ± 5 s around passing of the sensor line, individual passes, for a heavy (MB 2648, RT h) and a medium (YTV 2300, RT m) road tractor, loaded and unloaded. (Note that here the abscissa is in linear scale.)

a factor of 2–4; higher differences at larger distances are thus probably rather a consequence of differing propagation conditions. In particular:

- Tanks driving on terrain produce roughly the same seismic amplitude as when driving on a hard road.
- A tank with steel-only tracks (the Eastern T 55) causes about the same amplitude as types with rubber pads on the track elements (the Western Leopard 1 and M 48).

Optimum power-law fits for the different tank types or sites result in distance exponents of -1.0 for the T 55, and -2.0 to -1.5 for the M 48 and Leopard 1, if the respective sensors at the road margin (3.1 or 4.5 m) are excluded. This again underscores the variability found with seismic signals.

Fig. 7b shows peak seismic amplitudes of loaded and unloaded road tractors versus speed at 11.8 distance, occurring within ± 5 s around passing of the sensor line at the Amersfoort experiment. Usually, the peak values stem from the trailer, the amplitudes from the tractor are weaker. Both tractors behaved differently when the load was added. The peak amplitude of the heavy road tractor generally increased when the trailer of 23 Mg mass was loaded with a Leopard 1 main battle tank of 41 Mg. With the medium tractor, on the other hand, adding the load (an armoured personnel carrier YPR 765 of 11 Mg mass) to the trailer of about 10 Mg rather decreased the amplitude. Both types show a few exceptions and marked variation.

4.2. Detection ranges from amplitudes, sensor spacing

Using the decrease of amplitude with distance, acoustic and seismic detection ranges can be estimated for the simple criterion of the signal amplitude rising above background times a certain S/N factor, without spectral analysis or other sophistication. At Amersfoort, with a road in 800 m distance, acoustic background amplitudes during the day, without strong wind or other noise, were around 0.04 Pa (r.m.s. level around 58 dB re. 20 μPa), seismic ones were around 2 μm/s. With an S/N factor of 2, detection thresholds become 0.08 Pa and 4 μm/s—this would result in relatively many false alarms, but then spectral analysis, etc. could be started to sort out events. Fig. 5a shows that an acoustic threshold of 0.08 Pa is crossed for the medium truck and medium road tractor at about 60 m. For the louder vehicles, extrapolation would lead to several hundred metres or even kilometres—the latter range is, however, unrealistic under certain conditions, e.g., when wind shear refracts sound upward, away from the ground. A seismic-amplitude threshold of 4 μm/s is reached by the medium truck at 40 m, whereas extrapolation for the road tractors points to about 100 m, and for the tracked vehicles clearly above 100 m (but much closer than extrapolated in the acoustic case). Thus, rule-of-thumb detection ranges, solely from acoustic and seismic amplitudes at normal speeds, are about 50 m for medium trucks and medium road tractors, and 100 m or more for heavy road tractors and tracked vehicles. Similar results were found at a later experiment [30]. At quieter sites, lower thresholds with higher ranges will be possible.

Evasion scenarios have to be analyzed separately. Concerning very slow speed, Fig. 6 indicates reductions by factors about 0.5 and 0.7 of acoustic and seismic amplitude, respectively, when the medium road tractor (the medium truck is similar) moves with 2 m/s instead of 5 m/s. With Fig. 5, this leads to reduced detection ranges of about 30 and 20 m, respectively. For the heavy road tractor, about 130 and 80 m result, and the tracked vehicles remain clearly above 100 m.

Fig. 5a shows that masking of a quieter vehicle by a louder one is possible. E.g., the sound–pressure amplitude of a main battle tank at 100 m distance is about the same as the one from a medium road tractor or truck at 3 m. Masking could be effective if the tank signal were, say, 10 times higher than the truck one. This can mean that detection of a truck at 100 m could be made impossible by a tank at about 500 m (by extrapolation). This was indeed a problem during many of the truck measurements at the Amersfoort experiment: tanks moving at several 100 m distance, beyond the farthest sensors, produced considerable background noise, above which the truck signals rose only within, say, 30 m of the sensors, thus the truck signal dominated only for a short period at the sensors closest to the road, and not at all for the more distant ones. For seismic masking, about the same considerations apply as with acoustic signals.

The sensor (or sensor-pair) spacing in a control line can be derived from a minimum detection range of 50 or 100 m (depending on the vehicle types envisioned) for both acoustic and seismic signals. Applying a safety factor of 2 would lead to a spacing of 50 or 100 m, guaranteeing that each pass across the line would be sensed at at least two sensor positions, and at more for the noisier and heavier vehicles. More detailed analysis may allow for an increased spacing in certain scenarios. Whereas masking by loud vehicles at several hundred metres from the line could be frustrated by spectral analysis, it seems prudent that it should be avoided at all. Vehicle or other signals clearly above the detection threshold should provoke an alarm in any case. Control lines should thus stay at several hundred metres from roads with heavy-vehicle traffic, and special

regulations would have to cover cases when heavy vehicles have to move more closely. E.g. a farmer's tractor or wood-transport trucks would have to be announced in advance, and inspectors may need to be present for the whole duration of the activity close to the control line.

5. Spectra

5.1. Single spectra

Acoustic as well as seismic signals of heavy vehicles are more or less periodic. Thus, their spectra should consist mainly of lines at discrete frequencies—a fundamental frequency which is the inverse of the (quasi-)period, and its integer multiples, the harmonics. One source of periodicity is the engine, it is present with all vehicles and produces mainly noise, with the exhaust as the dominant source. The engine period, i.e., the duration after which engine events repeat, is one crank-shaft revolution for a two-stroke engine, and two revolutions for a four-stroke type. For tracked vehicles, periodic noise is also produced at the track, most strongly at the drive sprocket wheel. Periodic seismic excitation is produced directly via a track or a coarse-treaded tyre, and indirectly by acoustic-seismic transfer from periodic sound. A potential additional source is road-roughness-induced vibration of wheels or the vehicle body.

Power spectra were calculated by 1024-point fast Fourier transform with Hann window and periodogram normalization over intervals of 0.84 s or 0.42 s, depending on sampling rate. Fig. 8 shows acoustic and seismic spectra of a main battle tank at 11.8 m distance, taken around the time when it passed the sensor line. Due to a vanishing radial velocity component, Doppler shifts are negligible here. Both spectra consist mainly of two different harmonic series. The engine series with 19.65 Hz fundamental frequency dominates the acoustic spectrum (a). Because the Leopard-1 engine is of the four-stroke type, one engine period of 50.9 ms equals two crank-shaft revolutions, thus the revolution rate was 39.30 Hz = 2358 min^{-1}. In the spectrum shown, the fifth and seventh multiples are the strongest ones, with the seventh slightly higher. Spectra before and after the passing, however, have the fifth multiple as the strongest. This holds for most of the time for all passes; it has to do with the 10-cylinder V-type engine with two exhausts (see Section 5.3). The acoustic contribution at the track frequency and its harmonics is smaller.

The second series at $\nu_{0t} = 23.78$ Hz fundamental frequency dominates in the seismic spectrum (b) and can thus be identified as caused by the track. With the track-element length of the Leopard 1 of $l_t = 0.160$ m, it corresponds to a theoretical speed of $v_{\mathrm{th}} = l_t \cdot \nu_{0t} = 3.805$ m/s. From the light-beam interruption devices at $x = 0$ and 10 m the actual speed was 3.902 m/s. Such an error in track-frequency-derived speed by -2% to -3% was generally observed with the tracked vehicles at Amersfoort [21]. It can be explained by slight forward slip of the track while lying on the road—this behaviour is counter-intuitive, but was visually confirmed. In the seismic track series, the second multiple is the strongest here. This was observed generally with tracked vehicles at lower speeds; at higher speeds, mostly the fundamental frequency was the strongest on passing. The acoustically coupled vibration at the engine series is weaker than the track excitation most of which is produced directly.

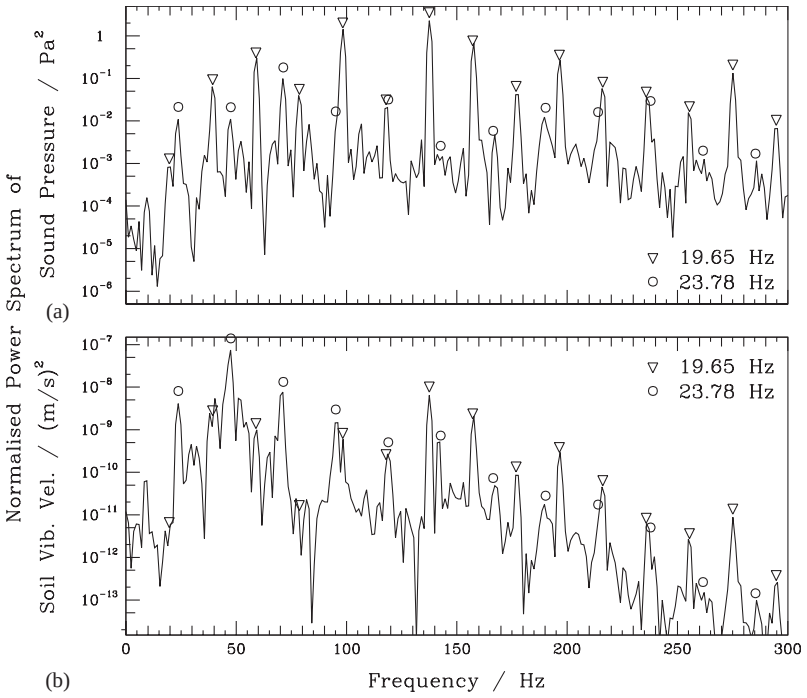

Fig. 8. Acoustic (a) and vertical seismic (b) power spectrum at 11.8 m distance when a Leopard-1 main battle tank just passed the sensor line ($x = 0$ m). The pass is the one of Figs. 2 and 3 ($v = 3.9$ m/s, direction east), the 0.84-s interval for spectrum calculation contains the one shown in Fig. 3. Symbols (engine: triangles, track: circles) mark all integer multiples of a fundamental. Filter frequencies 300 Hz both.

When plotting the crank-shaft rotation rate, derived from the engine frequency, versus the vehicle speed which for tracked vehicles can be gained from the track frequency, for most vehicles the passes form groups along the lines given by the gear ratios in the respective gears [21].

The track series in the acoustic, or the engine series in the seismic spectrum, show that the fundamental need not be strong or present as a line at all. Whenever there are sufficient instances where neighbouring (e.g., fifth and sixth) multiples exist, the frequency difference defines the fundamental frequency, and a higher-integer (2, 3, …) multiple of it cannot explain the series. Fundamental frequencies were mostly optimized interactively using a spectrum graph on the PC screen with mobile markers for the harmonics [33]. In this process, operator experience as well as plausible ranges for engine and track frequencies play a role. With some vehicles, assignment from one spectrum only was often difficult, e.g., the two-stroke armoured personnel carrier M 113 and its derivative YPR 765. Here, considering a full spectra sequence often helped, see Fig. 9. An automatized algorithm of fundamental-frequency finding works in many cases [34,30].

Acoustic spectra of wheeled vehicles consist mainly of the engine series, multiples have been observed to 1 kHz. For some vehicles, there are a few prominent lines outside of the series. Seismic spectra of wheeled vehicles usually contain lines at the frequencies of the acoustic lines, plus somewhat irregular broad features in the range 10–50 Hz.

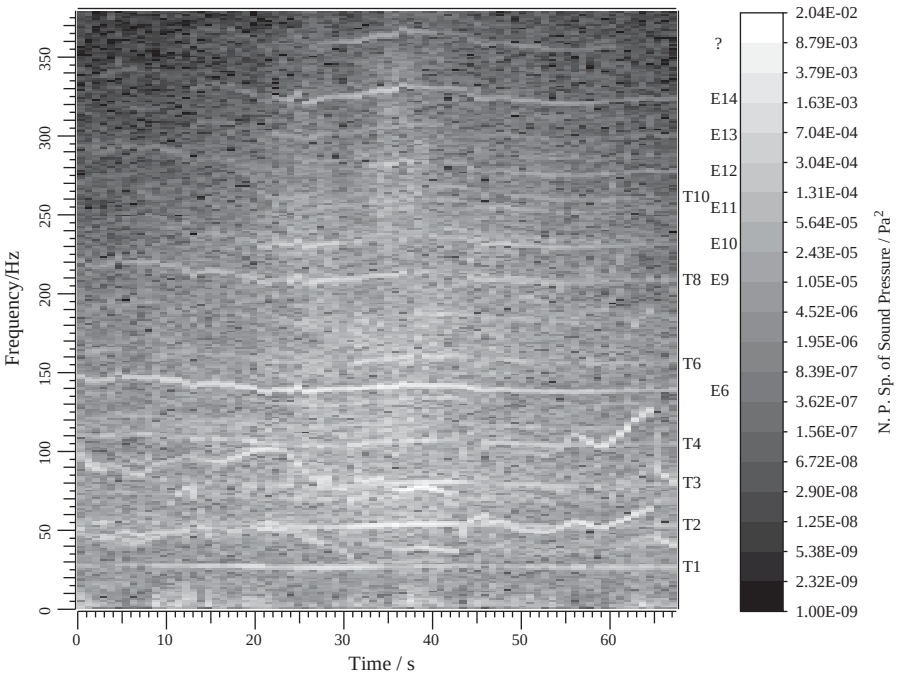

Fig. 9. Acoustic spectra sequence at 40 m distance from the lane centre during a pass of the YPR-765 armoured personnel carrier with 4.0 m/s in direction east (1024-point Fourier transform with Hann window, periodogram normalization, adjacent 0.84-s intervals). Spectral power is coded in grey value (logarithmic scale, see bar at right). The vehicle moved from about $x = -140$ m to about $x = 130$ m during the time period shown, the sensor line was passed at $t_0 = 35.5$ s. Multiples of the track fundamental frequency (about 26 Hz), and of the engine frequency (about 23 Hz), are marked T resp. E at the right. The source of the line at about 360 Hz, at 15.5 times the engine frequency, is unclear. The two additional lines with strongly varying frequencies between 30 and 130 Hz probably stem from another vehicle moving irregularly at a few 100 m distance. Filter frequency 300 Hz.

5.2. *Spectra sequence*

Fig. 9 shows the sequence of acoustic spectra at 40 m distance during a pass of the YPR-765 armoured personnel carrier. Because the engine of this vehicle is much less noisy than that of a main battle tank, the track noise is relatively stronger. This makes finding the engine series in single spectra difficult. In the experiment, speed (4.0 m/s) and track-element length (0.15 m) are known; this helps to find the track fundamental frequency of about 26 Hz. Of the track series, multiples 1–4, 6, 8, and 10 can be identified. The engine series (about 23 Hz fundamental frequency) is present in the dominant sixth multiple; further visible are the nineth to 14th multiples. Because the engine rotation rate and speed varied somewhat during the pass, the slow change of Doppler shift at the 40-m microphone cannot be seen here (but is evident with other passes and vehicles). Lines of the track and engine series run at constant mutual frequency ratios, according to the gear used. Track multiple 8 has the same frequency as engine multiple 9, about 210 Hz, thus this line cannot be unambiguously assigned to one or both series. There is one clear YPR-765-related line at about 360 Hz (already strongly attentuated by the low-pass filter) which

is 15.5 times the engine frequency (and 13.8 times the track frequency). Most probably it has to do with the engine; because there are no other lines at odd multiples, the assigned engine frequency is not divided by two. Why this occurs requires further study.

Fig. 9 demonstrates the problem that multiple vehicles present. Superposed on the lines of the measured vehicle of about constant frequency are two other lines with comparable or even higher power the frequencies of which vary strongly with time. Their mutual frequency ratio is 2.0 throughout. At 43 and 65 s, the gears were changed obviously. These lines probably stem from a heavy vehicle which operated at a few 100 m distance from the experiment. The absolute frequencies suggest that they are the third and sixth multiple of its engine series which would fit to six cylinders (see Section 5.3).

Looking only at a single-interval spectrum can give confusing results. Whenever a line-frequency ratio varies with time, as, e.g., in the case of two independent vehicles, a two-dimensional plot showing the time course of their frequencies can help to sort out which line belongs to which series, and to find time intervals when the lines do not overlap. In these intervals then single-spectrum analysis, as shown in Fig. 8, can be used to assign even the weaker lines which are not evident in the two-dimensional grey-scale images.

Beside considering different times, separation of distinct sources can also make use of multiple sensors. At different positions, signals will be sensed with different amplitudes, according to the respective source distances and orientations. This was done successfully by visually comparing spectral sequences from different sensors. Devising a reliable algorithm for such a process will probably be a complex task, however, in particular when it has to work with unknown vehicles and speeds.

5.3. Dominant engine harmonic, number of cylinders and exhausts

If each cylinder firing would lead to one narrow overpressure pulse at the mouth of one single exhaust, n overpressure- and gas-efflux pulses per engine period would be expected at the outlet if the n cylinders are ignited sequentially. Since acoustic-wave sound pressure is proportional to the time derivative of the efflux rate [35], this would lead to n overpressure-underpressure events per period, propagating into all directions. As a consequence, the dominant signal frequency at all locations should be n times the engine frequency v_E. Thus, the strongest multiple in the engine series should be the nth in this theoretical, simple case.

To find out whether, and under which conditions, this assumption is true, vehicle passes of the Amersfoort experiment were examined. Acoustic spectra were computed around the time of passing the sensor line for the microphone at 11.8 m; the number of the strongest multiple in the engine series was determined and plotted versus the engine rotation rate. Fig. 10 shows the results. The two vehicles with one exhaust behave as the simple model suggests at practically all rotation rates; these are the armoured personnel carrier YPR 765 with a 6-cylinder V-type engine (b) and the medium road tractor DAF YTV with a six-cylinder in-line engine (d). Other vehicles with one exhaust were similar, but not all of them and not under all conditions, see Table 5.

The YPR 765 poses specific difficulties: it is the only vehicle with a two-stroke engine, and the engine lines are weaker than the track ones. During these evaluations this vehicle has become notorious for inconsistent spectra with lines and series difficult to find and assign; in this respect it is similar to the U.S. APC M 113 of which it is a derivative (see also Fig. 9, Table 5, and [29]). In

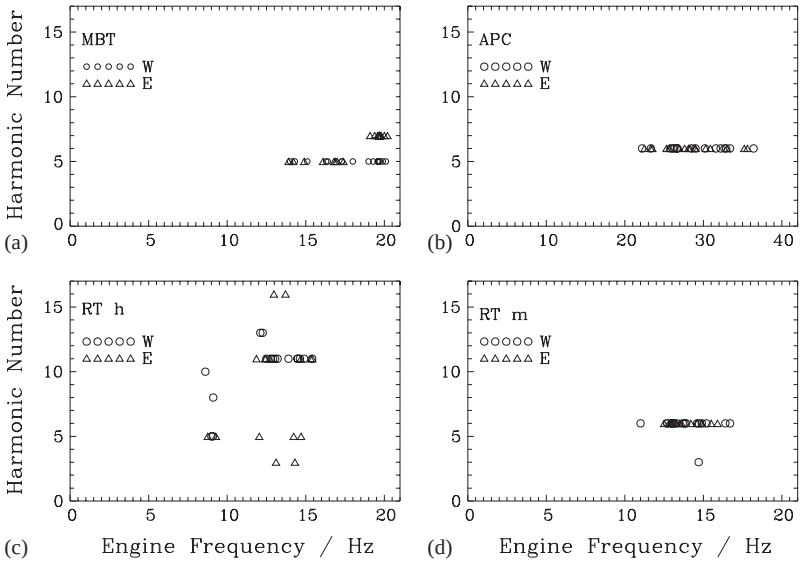

Fig. 10. Number of the strongest multiple in the acoustic engine series at 11.8 m distance during passing of the sensor line versus engine rotation rate, for vehicles of the Amersfoort 1992 measurements. (Spectra by 1024-point Fourier transform with Hann window, periodogram normalization, 0.84-s interval). The driving direction is indicated; the microphone was south of the road (see Fig. 1), thus it was at the left for western (W) passes, and at the right for eastern (E) passes. Gaps in rotation-rate coverage are a consequence of the speed steps asked for and the gears chosen by the drivers. (a) Main battle tank Leopard 1 (V10 engine, 2 exhausts, 4 stroke), (b) Armoured personnel carrier YPR 765 (V6 engine, 1 exhaust, 2 stroke), (c) Heavy road tractor MB 2648 (V8 engine, 2 exhausts, 4 stroke), (d) Medium road tractor DAF YTV 2300 (in-line six-cylinder engine, 1 exhaust, 4 stroke). Note that the frequency scale in (b) is different by a factor 2, compensating for the two-stroke engine; thus, engine rotation rates are plotted at equal positions throughout.

the present work, several of the series/fundamental-frequency assignments done in Ref. [21] on the basis of one single-interval spectrum around the passing time were corrected by considering the sequence of spectra of the complete pass; in addition, spectra from more distant microphones were used to find and discard lines from distant louder vehicles, see Section 5.2.

The vehicles with two exhausts showed different behaviour. The main battle tank Leopard 1—with a 10-cylinder, V-type engine where each group of five cylinders leads to one lateral exhaust—has mostly the fifth multiple dominating; exceptions are at high rotation rates with the microphone on the right hand side, where the seventh multiple dominates (Fig. 10a). Similar behaviour, that is the number of the strongest multiple equal to half the number of cylinders, was also observed for other vehicles with a V-type engine and two exhausts, as shown in Table 5.

However, the heavy road tractor MB 2648 provides a counter-example (Fig. 10c). This vehicle has an eight-cylinder, V-type engine with two exhausts. Here, the eighth multiple is never the strongest one, and the fourth only very rarely. Instead, the 11th multiple is the highest mostly, with the orders 5, 3, 13, and 16 occurring sometimes. The reason for this irregularity and for the preponderance of numbers which have nothing to do with 8 is unclear at present.

Strongest-multiple numbers of many vehicle types are presented in Table 5, together with the engine class with cylinder arrangement and exhaust number. Most of the data stem from

Table 5
Number of the strongest multiple in the acoustic engine series for different vehicles (sorted by cylinder number), mostly from BVP experiments

Vehicle	Class	Engine type	Number of exhausts	Number of strongest multiple (sorted by frequency of occurrence)	Reference
M 48	MBT	V 12 P 4	2	6	[29,30]
T 55	MBT	V 12 D 4	1	3,12	[28,29]
Tatra T 815	RT	V 12 D 4	2	6,12	[28,29]
Leopard 2	MBT	V 12 D 4	2	6,3;9,12[a]	[30]
Leopard 1	MBT	V 10 D 4	2	∗5,7	[21,30]
Magirus Deutz 320	RT	V 10 D 4	1	3,5,7[b]	[29]
Jaguar	TDM	V 8 D 4	1	8,6	[30]
Fuchs	AGPC	V 8 D 4	1	8	[30]
Mercedes Benz 2648	RT	V 8 D 4	2	∗11, others	[21], this work
Formula-1-like racing car	RC	V 8 P 4	2	4	[36]
YPR 765	APC	V 6 D 2	1	∗6[c]	This work
M 113	APC	V 6 D 2	1	6,3	[29]
DAF YTV 2300	RT	L 6 D 4	1	∗6	[21]
DAF YA 4440	L	L 6 D 4	1	3,1[d]	This work
MB 1017	L	L 6 D 4	1	3, seldom 6[a]	[30]
Praga V3S	L	L 6 D 4	1	6,12	[28,29]
Hermelin	RV	L 6 D 4	1	6,12	[30]
Unimog	SL	L 6 D 4	1	3,6[a]	[30]
Mercedes Benz[e]	L	L 4 D 4	1	4	[37]

Observation mostly laterally, only for the Amersfoort 1992 experiment of the BVP systematic analysis of many speeds/rotation rates was done (asterisk in fifth column, Ref. [21], this work). Note that in many cases the strongest-multiple number is equal to the number of cylinders or its half. Vehicle class: MBT: main battle tank; APC: armoured personnel carrier (tracked); TDM: tank destroyer, missile (tracked); AGPC: armoured general-purpose carrier (wheeled); RT: road tractor; L: lorry; RC: racing car; SL: small lorry; RV: reconnaissance vehicle. Engine type: L/V: in-line/V-type cylinder arrangement, number of cylinders P/D: petrol/Diesel, number of strokes.

[a] Corrected for error in Ref. [30] (Leopard 2: 6 missing; MB 1017—Unimog: harmonics exchanged).

[b] Not ordered by frequency of occurrence.

[c] Ref. [21] had reported multiples 6, 3; in-depth re-investigation led to re-assignment of the engine series in several cases after which the sixth multiple was the strongest throughout.

[d] Only one pass tested.

[e] Name of vehicle not specified in the article.

experiments of the BVP, but other observations of a racing car and an unspecified lorry were added. For the Amersfoort 1992 experiment, many speeds and rotation rates were evaluated systematically, with the sensor(s) lateral of the vehicle (see Fig. 10). For the other experiments, only a limited number of rotation rates were available.

What are possible reasons why the cylinder-firing rate should not be the dominant sound frequency emitted? Inside the exhaust, acoustics are fairly complicated, with reflections arising at many places, different distances from the outlet valves to the exhaust orifice, and non-linear effects [11]. Pressure pulses from individual cylinders could merge if their duration—with

echoes—is long enough and the firing frequency high enough. Outside, pulse merging is conceivable with superposition of signals from more than one exhaust if pulse durations are similar to the propagation-time differences. Intake noise may also contribute.

Obviously more research is needed to understand the interaction between cylinder number and the number of the strongest multiple in dependence of engine class, rotation rate and observation direction. An empirical rule of thumb is that these numbers are often equal, or the latter is often half the former. Conversely, from the strongest-multiple number observed in the acoustic spectrum of an unknown vehicle, a good guess on the cylinder number is possible by taking that number or its double—keeping in mind, however, that such a guess may be wrong for some vehicles or under some conditions.

6. Special aspects

6.1. Sensor-array processing

Signals from multiple sensors can be used to derive more information about a source. One method is beam forming: assuming that one plane wave (source at large distance) propagates with a certain velocity in a certain direction across an array of sensors, each one senses essentially the same signal, but time-shifted according to the respective position. If the signals are shifted backwards by the correct propagation delays and summed, they superpose coherently. If the time shifts do not fit to the actual wave direction and velocity, signals fit worse and the sum amplitude is smaller. The sensor array forms an antenna with a receiving beam. Beam forming can be used to reduce background noise from other directions or arriving with other velocities, and can thus help to separate distinct sources. For unknown propagation velocity v and direction φ, v and φ are varied systematically; the resulting two-dimensional distribution of sum-signal amplitude will show a peak around the correct values of v and φ which can thus be estimated. For the amplitude, the r.m.s. value of the average signal is used (sum divided by number of signals). Only the basic results of one vehicle are described.

With acoustic signals, beam forming works well, as demonstrated in an example from a pass of the Leopard-1 main battle tank with -6.2 m/s speed. Signals of 0.2 s duration of a three-microphone array 40 m from the lane centre, mutual distance 0.9–1.7 m, were analyzed. When the waves were produced, i.e., taking into account the sound-propagation time, the vehicle centre moved from $x = 31.6$ to 30.4 m, i.e., before it passed the zero line at 36.28 s. The direction from that position to the array is $\varphi = 232^\circ$. The wave-velocity magnitude was varied between 100 and 700 m/s and the direction from 0 to 350°. Fig. 11 a shows the r.m.s. value of the average array signal versus the x and y components of wave velocity. There is one broad peak with a maximum at 330 m/s and 230°. These values fit well to the sound speed of 338 m/s for 10°C temperature and the direction from the vehicle to the array. The signals—after shifting in time according to the maximum—are very similar and actually superpose coherently, as shown in Fig. 11b. In this example, cross-correlation coefficients between the sensors were above 0.98.

At other times of the pass, there were similar peaks with wave speeds of 290–380 m/s, fitting to the speed of sound, and the direction angle changed with the orientation of the vehicle—typically it was a few degrees off, maximally 15°. Cross-correlation coefficients were above 0.9 throughout.

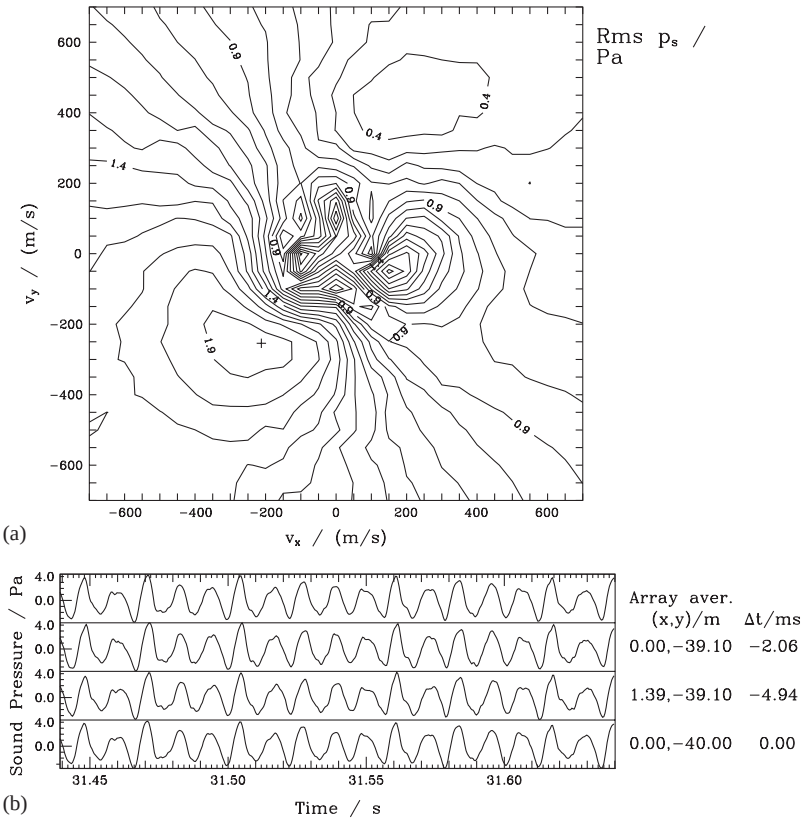

Fig. 11. Example of sensor-array evaluation for acoustic signals. Three microphones about 40 m off the lane centre recorded a pass of the Leopard-1 main battle tank with −6.2 m/s (direction west). Filter frequencies 1 kHz. Interval duration 0.2 s. The direction from the vehicle to the array was $\varphi = 232°$. (a) R.m.s. value of average signal of sensor array versus x and y components of assumed plane-wave velocity across the array, contour plot; minimum value 0.3 Pa. The maximum of the broad peak around (−210, −250) m/s is 1.96 Pa at $v = 330$ m/s, $\varphi = 230°$, indicated by a cross. (b) Signals of the three microphones, shifted according to the maximum of (a) (lower three curves), and resulting array average (uppermost curve). Sensor co-ordinates and time shifts are shown on the right, height was 0.2 m for all.

This is a general experience: absent disturbances from other sources, acoustic signals at neighbouring sensors are time-shifted versions of each other, so that the assumption of one plane wave travelling with one single wave velocity is usually justified. Thus, the wave velocity and the direction from the source can be estimated by beam forming (or cross-correlation [38]). Sharper peaks and thus better resolution in wave velocity and direction are expected if more sensors are used, if the array size is increased (still remaining in the plane-wave case, i.e., array dimension small compared to distance from the source), and/or if the signals are recorded at higher bandwidth.

With seismic signals, on the other hand, the situation is very different. Signals at neighbouring geophones are not just time-shifted versions of each other, but differ widely, see Fig. 4 and the explanations in Section 3. Thus, there is no wave-velocity vector at which coherent superposition of the shifted signals can take place. Seismic beam forming was tried using signals of 10 geophones within an 11-m diameter circle about 40 m from the lane centre for the pass and time of Fig. 11.

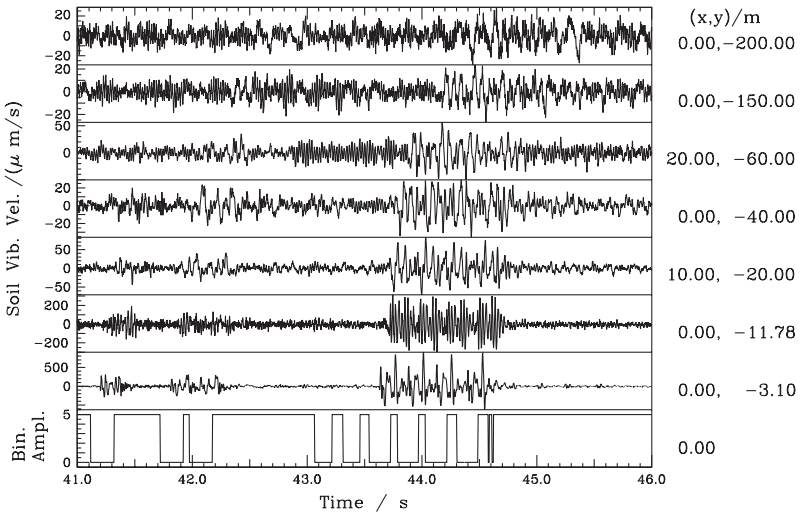

Fig. 12. Vertical seismic signals at 3.1–200 m distance from the lane centre when an unloaded heavy road tractor MB 2648 rolled over a steel plate of 2 cm thickness and 0.4 m width, lying at $x = 0$ m, $y = -1$ m, with its sensor-facing wheels. The speed was -5.2 m/s (direction west). Geophone co-ordinates are given on the right. Filter frequencies 300 Hz. The lowest curve shows the signal of the light-beam interruption device at $x = 0$ m, height 0.3 m.

There were several low maxima of the array-signal amplitude at inconsistent velocity-direction pairs. With cross-correlation coefficients between 0.2 and 0.8, the signals give no clear indication of one wave passing the array. At other times for this pass, the picture was the same. Similar behaviour had been observed with other vehicles and other experiments [29].

6.2. Seismic signal from bump in the road

It is to be expected that the seismic amplitude from a driving vehicle increases with road roughness. In order to get some estimate on the strength of this effect and to get a sense of how pulse-like seismic excitation propagates, some passes were done with a 2 cm thick and 0.40 m wide steel plate on the road. The plate was rolled over by the wheels of the sensor-facing side. For such a pass across the plate by the heavy road tractor (unloaded, 5.2 m/s speed) at the Amersfoort experiment, Fig. 12 shows the seismic signals recorded in various locations. The plate was about 1 m off the lane centre, centred at $x = 0$ m, thus the geophone on the road margin, at $x = 0$ m, $y = -3.1$ m, had about 2 m as closest distance to the source. The lowest curve is the light-beam signal at $x = 0$ m; here the $1 + 2$ interruptions by the tractor wheels are clearly seen, as are the 6 interruptions by the trailer wheels. At the closest geophone each wheel touching the ground produces a wave train with 4–5 major pulses. These pulse trains show some similarity, so that individual axles can principally be discerned and counted. (Note that for the empty trailer the first two axles had been raised which is nicely confirmed here by the shorter interruption durations and missing seismic signals.) Similarity of the individual-axle signals already starts to get lost at 11.8 m distance, and deteriorates further at larger distances, probably due to wave dispersion and consequent signal overlap in time.

The seismic amplitudes from the bump were compared with the maximum ones from driving with similar speed on the smooth road, i.e., from passes without bump, which occurred at comparable times. The ratios between both are 7.3, 3.5, 4.4, and 3.0 at distances 3.1, 11.8, 20, and 40 m, respectively, for the trailer axles (producing the highest signal). Amplitudes predicted from an empirical model ([14,15], parameters for sand/gravel), are mostly above the values caused by the tractor and below the ones from the trailer, by up to a factor 2.

In the Doksy 1989 experiment, the same plate had been used. At a speed of 11 m/s, the amplitudes at 4.5 m distance (slightly off the road margin) were higher by a factor 3 for a similar heavy road tractor (Tatra 815, unloaded). At the same speed, however, signals from a medium truck and a light van were 20 and 30 times stronger, respectively, than when driving on the asphalt road without bump [28].

A safe conclusion is that seismic excitation is strongly increased by small obstacles or general road roughness. With single bumps, at close distance axle counting becomes possible. Future work should investigate if for known speed, the axle load can be estimated from the seismic amplitude.

7. Conclusion and outlook

The Bochum Verification Project has carried out a series of four open, international experiments measuring acoustic and seismic signals produced by heavy military vehicles of different types, under different conditions and at several distances. Evaluation as of now has brought the following results:

Acoustic and seismic sensors will be useful for co-operative verification of disarmament and peace-keeping agreements. They can detect heavy military vehicles passively, independent of weather and daylight.

Acoustic as well as seismic signals of such vehicles contain contributions from the engine which usually dominate in the acoustic signal. With tracked vehicles, there are additional components produced by the track; these dominate the seismic signal at short-to-medium distances.

Acoustic amplitudes immediately beside a passing vehicle, about 3 m from the lane centre, are about 10 Pa for trucks, and 30–80 Pa for tracked vehicles. Seismic amplitudes vary more strongly, between about 1 mm/s for trucks and 10–20 mm/s for tracked vehicles. Variations by a factor of 2 and more occur in both acoustic as well as seismic amplitudes; this makes evaluation of subtle differences using amplitudes difficult.

The acoustic amplitude varies roughly proportionally to the inverse distance, with the signal keeping its shape. For the seismic signal, the decrease with distance is rather irregular, depending on local conditions; overall, power-law fits gave optimum distance exponents between -2 and -1. Due to different wave types and dispersion, together with acoustic-to-seismic coupling, the seismic signal changes its form even over short range. Under conditions of moderate background activity, amplitude detection thresholds of 0.08 Pa for sound pressure, and 4 μm/s for soil vibration velocity, may be appropriate. For both sensor types these values lead to detection ranges at normal speeds of about 50 m for medium trucks, about 100 m for heavy road tractors, and several times that value for tracked vehicles. Thus, a 50-m or 100-m spacing, respectively, of pairs of

microphones and geophones along a monitored line will normally provide redundant detection of covert trespassing at least at two, and often four or more positions.

Heavy-vehicle spectra consist mainly of lines which form series at a fundamental frequency and its harmonics. The engine series exists with all vehicles; the fundamental frequency—not always present as a line—is equal to the engine rotation rate (for two-stroke engines) or its half (for four-stroke engines). For tracked vehicles, the track produces an additional series with a fundamental frequency approximately equal to the vehicle speed divided by the track-element length. In the acoustic channel, it is mainly produced by the drive sprocket gripping into the gaps between the track elements; in the seismic channel, it is primarily caused by the road wheels rolling over the track elements.

In acoustic spectra, the order of the highest harmonic of the engine series is often equal to the number of cylinders of the engine, or half that number. Thus, a simple estimate of cylinder number can be gained from the highest harmonic; however, this estimate need not be correct in all cases.

Sensor-array processing by beam forming works well in the acoustic realm, due to the similarity of signal form measured at different locations. Conversely, seismic beam forming gives bad results, because the seismic signals are dissimilar even at neighbouring positions.

A 2-cm bump in an otherwise smooth road resulted in a seismic-amplitude increase by a factor of 3–7 for a road tractor at 5 m/s speed.

Production and propagation of heavy-vehicle signals are complicated processes, in particular in the seismic case. Usually, there are several sources and several paths along which excitation can propagate to a sensor, including transfer from acoustic to seismic waves. Future work should try to model and understand these processes. For the monitoring application, recognition of vehicle type would be very useful. This seems most promising with the acoustic signal, focusing on the engine contribution [30]. Advanced work should deal with separation of multiple sources and several types of multi-sensor processing, from source localization to fusion of information from different sensor types, in order to derive as much information on a vehicle and its trajectory as possible.

Acknowledgements

Over the years, the research of the BVP has been funded by grants from the Volkswagen-Stiftung (Germany), the John D. and Catherine T. MacArthur Foundation (U.S.A.), the Ministerium für Wissenschaft, Schule und Forschung of the German Federal State of Nordrhein-Westfalen, and the German Bundesministerium für Bildung und Forschung. This support is gratefully acknowledged. The author expresses his gratitude to the Ministries of Defence of the (then) CSSR and CSFR, the Federal Republic of Germany, and of the Netherlands for having given permission to carry out the experiments, and to the local units and soldiers who worked as organizers, drivers, etc.

References

[1] L.A. Dunn, A.E. Gordon, *Arms Control Verification & the New Role of On-Site Inspection—Challenges, Issues and Realities*, Heath, Lexington MA/Toronto, 1989.

[2] J. Altmann, On-site verification technologies—an overview, in: J. Altmann, H. van der Graaf, P.M. Lewis, P. Markl (Eds.), *Verification at Vienna—Monitoring Reductions of Conventional Armed Forces*, Gordon & Breach, New York, 1992, pp. 113–124.

[3] W.A. Huijssoon, Questionnaire answers analysis, in: J. Altmann, H. Fischer, H. van der Graaf (Eds.), *Sensors for Peace—Applications, Systems, and Legal Requirements for Monitoring in Peace Operations*, UN Institute for Disarmament Research/UNO, Geneva/New York, 1998, pp. 61–64.
[4] S. Koulik, The Sinai experience, in: R. Kokoski, S. Koulik (Eds.), *Verification of Conventional Arms Control in Europe—Technological Constraints and Opportunities*, SIPRI/Westview, Stockholm/Boulder CO, 1990, pp. 217–228.
[5] M.G. Vannoni, *Sensors in the Sinai—A Precedent for Regional Cooperative Monitoring*, Cooperative Monitoring Center, Sandia National Laboratories, Albuquerque, NM, 1996.
[6] J. Altmann, Verification techniques for heavy land vehicles using short-range sensors, in: J. Altmann, J. Rotblat (Eds.), *Verification of Arms Reductions—Nuclear, Conventional and Chemical*, Springer, Berlin, 1988, pp. 184–194.
[7] J. Altmann, B. Gonsior, Nahsensoren für die kooperative Verifikation der Abrüstung von konventionellen Waffen, *Sicherheit und Frieden* 7 (1989) 77–82.
[8] I. Oelrich, V. Utgoff, Confidence building with unmanned sensors in Europe, in: B.M. Blechman (Ed.), *Technology and the Limitation of International Conflict*, University Press of America, Lanham, MD, 1989, pp. 13–31.
[9] W. Baus, *Magnetic-anomaly detection using conventional and superconductive sensors with respect to vehicle monitoring*, Verification—Research Reports, No. 8, Brockmeyer, Bochum, 1995.
[10] P.M. Nelson (Ed.), *Transportation Noise Reference Handbook*. Butterworths, London, 1987 (Part 3, Road Traffic Noise).
[11] P.O.A.L. Davies, K.R. Holland, I.C. Engine Intake and Exhaust Noise Assessment, *Journal of Sound and Vibration* 223 (1999) 425–444.
[12] M.G. Pottinger, T.J. Yager (Eds.), *The Tire Pavement Interface*, ASTM, Philadelphia, PA, 1986.
[13] D. Cebon, *Interaction Between Heavy Vehicles and Roads*, 39th L. Ray Buckendale Lecture, SAE SP-951, Society of Automotive Engineers, Warrendale, PA, 1993.
[14] G.R. Watts, Traffic induced vibrations in buildings, *Transport and Road Research Laboratory* (*Crowthorne*) RR 246 (1990) 1–31 (cited after Crispino and D'apuzzo).
[15] M. Crispino, M. D'apuzzo, Measurement and prediction of traffic-induced vibrations in a heritage building, *Journal of Sound and Vibration* 246 (2001) 319–335.
[16] R. Blumrich, Technical potential, status and costs of ground sensor systems, in: J. Altmann, H. Fischer, H. van der Graaf (Eds.), *Sensors for Peace—Applications, Systems, and Legal Requirements for Monitoring in Peace Operations*, UN Institute for Disarmament Research/UNO, Geneva/New York, 1998, pp. 65–153.
[17] Swedish Defence Research Organisation FOA, *Seismology 1985* (FOA Rapport C 20605-T1) 1985; *Seismology 1986* (FOA Rapport 20662-9.1), 1986 (sections on ground sensor systems).
[18] D.G. Albert, The effect of snow on vehicle-generated seismic signatures, *Journal of the Acoustical Society of America* 81 (1987) 881–887.
[19] A. Güdesen, et al. Luft- und Bodenschallsensoren in der Wehrtechnik, in *Jahrbuch der Wehrtechnik*, Vol. 19, Bernard & Graefe, Koblenz, 1990, pp. 174–185.
[20] J. Altmann, Physikalische Forschung zur akustischen und seismischen Überwachung von Land- und Luftfahrzeug-Bewegungen für die Verifikation—ein Erfahrungsbericht, in: J. Altmann, G. Neuneck (Eds.), *Naturwissenschaftliche Beiträge zu Abrüstung und Verifikation*, Bad Honnef/Hamburg, Deutsche Physikalische Gesellschaft/Forschungsverband Naturwissenschaft, Abrüstung und internationale Sicherheit, 1996, pp. 178–202.
[21] W. Kaiser, *Sound and vibration from heavy military vehicles—investigations of frequency assignment and wave spreading with respect to monitoring under disarmament treaties*, Verification—Research Reports, No. 9, ISL, Hagen, 1998.
[22] T.F.W. Embleton, Tutorial on sound propagation outdoors, *Journal of the Acoustical Society of America* 100 (1996) 31–48.
[23] K. Attenborough, Review of ground effects on outdoor sound propagation from continuous broadband sources, *Applied Acoustics* 24 (1988) 289–319.
[24] M.G. Pottinger, et al., A review of tire/pavement interaction induced noise and vibration, in: M.G. Pottinger, T.J. Yager (Eds.), *The Tire Pavement Interface*, ASTM, Philadelphia, 1986, pp. 183–287.
[25] M.B. Dobrin, *Introduction to Geophysical Prospecting*, McGraw-Hill, New York, 1976.
[26] H. Militzer, F. Weber, *Angewandte Geophysik, Band 3: Seismik*, Springer/Akademie, Wien etc./Berlin, 1987.

[27] J.M. Sabatier, H.E. Bass, L.N. Bolen, K. Attenborough, Acoustically induced seismic waves, *Journal of the Acoustical Society of America* 80 (1986) 646–649.
[28] R. Alfier, J. Altmann, L. Anger, W. Baus, B. Gonsior, J. Hanousek, W. Kaiser, J. Klinger, J. Malek, M. Pospisil, V. Rudajev, I. Sabo, *Ground vibration and acoustic waves produced by land vehicles of the Warsaw Treaty Organization—results of the 1989 measurements at Doksy*, *CSFR*, Verification—Research Reports, No. 1, Brockmeyer, Bochum, 1990.
[29] J. Altmann, L. Anger, W. Baus, A. DeVolpi, B. Gonsior, J. Grin, J. Hanousek, V. Journé, W. Kaiser, J. Klinger, P. Lewis, J. Malek, J. Matousek, M. Pospisil, B. Rost, V. Rudajev, I. Sabo, P. Stein, *Ground vibration*, *acoustic waves and magnetic disturbance produced by land vehicles of the North-Atlantic Treaty Organization—results of the 1989 measurements at Baumholder*, *FRG*, Verification—Research Reports, No. 3, Brockmeyer, Bochum, 1993.
[30] J. Altmann, S. Linev, A. Weiß, Acoustic-seismic detection and classification of military vehicles—developing tools for disarmament and peace-keeping, *Applied Acoustics* 63 (2002) 1085–1107.
[31] C.M. Harris, *Handbook of Acoustical Measurements and Noise Control*, McGraw-Hill, New York, 1991 (Chapters 2, 17).
[32] M.J. Griffin, *Handbook of Human Vibration*, Academic Press, London, 1996 (Section 6.2).
[33] J. Altmann, S. Brosig, *MESS6/EVAL6—A versatile program for measuring and evaluating multiple sensor signals*, Verification—Research Reports, No. 6, Brockmeyer, Bochum, 1994.
[34] J. Altmann, Klassifikation von Kettenfahrzeugdurchfahrten mittels Linienserien in akustischen Spektren, in: *Fortschritte der Akustik—DAGA 97*, Deutsche Gesellschaft für Akustik, Oldenburg, 1997, pp. 232–233.
[35] P.M. Morse, K.U. Ingard, *Theoretical Acoustics*, McGraw-Hill, New York, 1968 (Section 7.1).
[36] M. Pomierski, Ermittlung der Motordrehzahlen von Rennwagen aus dem Vorbeifahrtgeräusch, in: *Fortschritte der Akustik—DAGA 91*, DPG GmbH, Bad Honnef, 1991, pp. 397–400.
[37] D. Hackenbroich, Rechnerische Untersuchung des Auspuffmündungsgeräuschs bei Nutzfahrzeugen mit Hilfe von Rohrströmungs- und Finite-Element-Programmen, in: *Fortschritte der Akustik—DAGA 90*, DPG GmbH./IAP-TU, Bad Honnef/Wien, 1990, pp. 405–408.
[38] R. Blumrich, J. Altmann, Medium-range localisation of aircraft via triangulation, *Applied Acoustics* 61 (2000) 65–82.